Numerical modeling of Gauss monocycle pulse in transient acoustic field

Lukáš Koudela, Jindřich Jansa, Pavel Karban
University of West Bohemia
306 14 Plzen, Univerzitni 26, e-mail: {koudela, jansaj, karban}@kte.zcu.cz

Digest: Numerical solution of acoustic wave equation in the time domain is performed. The mathematical model is described by the partial differential wave equation supplemented with appropriate boundary conditions. The goal is to obtain the time evolution of the distribution of acoustic pressure, which can serve as the basis for the solution of various subsequent problems. The paper discusses the results of the numerical analysis of the Gauss monocycle pulse that proceeds from the signal source and incident on the semi-circular acoustic diffuser in a free field, realized by a fully adaptive higher-order finite element method implemented in codes Agros2D and Hermes developed by the *hp*-FEM group. Selected results of the computations are compared with the data obtained by the commercial code COMSOL Multiphysics.

KEYWORDS: Gauss monocycle pulse, acoustic transient field, finite element method.

1. Introduction

There exist numerous acoustic problems where knowledge of only steady state or harmonic acoustic field is insufficient. In such cases it is necessary to solve more complicated transient phenomena, which is typical for room acoustics. Of great importance are, for example, reflected sound waves produced by an acoustic diffuser which is an acoustic element that uniformly disperses sound regardless of the angle of incidence. It is used to adjust the sound level distribution in the concert halls, theatres or areas that require perfect acoustics. Due to the fact that the design and measurement of diffusers is very complicated and expensive, numerical modelling could be an effective alternative of solving such tasks in this field. From the viewpoint of numerical modeling, it is necessary to define the test signal for determining the suitability of the acoustic diffuser. In this field, the Gauss monocycle pulse is mostly used, so it is also needed to be able to model this type of signal [1].

2. Mathematical model

The continuous mathematical model of the problem is given by the corresponding non-stationary partial differential equation supplemented with appropriate boundary conditions. The wave equation will be derived from the

Newton law of motion, continuity equation and equation of state for the adiabatic processes [2].

The mathematical model is defined for ideal fluid with the properties of a perfect continuum. In this case we consider several simplifications. All dissipative effects and internal forces acting on the particles are neglected, the continuum is assumed as homogeneous, isotropic and perfectly elastic and the velocity is considered small.

Newton's law of motion is used in the form of a highly simplified Navier-Stokes equation for compressible fluids with neglected viscosity and external forces acting on the particles. The equation will be used in the form of

$$\rho \frac{\partial \boldsymbol{v}}{\partial t} = -\text{grad}\ p, \tag{1}$$

where the symbol ρ stands for the specific mass, $\boldsymbol{v}$ represents the velocity, t is time and p denotes the acoustic pressure.

The other mentioned equations are the continuity equation

$$\text{div}(\rho \boldsymbol{v}) + \frac{\partial \rho}{\partial t} = 0, \tag{2}$$

and state equation for adiabatic processes

$$p \cdot \rho^{-\kappa} = C, \tag{3}$$

where κ is the Poisson ratio (for air $\kappa = 1.4$) and C is a suitable constant.

The derivation starts from the application of operator divergence to equation (1)

$$-\text{div}\left(\frac{1}{\rho}\text{grad}\ p\right) = \frac{\partial}{\partial t}\text{div}\ \mathbf{v}. \tag{4}$$

The next step is the substitution of the equation (2) into the right-hand side of (4)

$$-\text{div}\left(\frac{1}{\rho}\text{grad}\ p\right) = -\frac{1}{\rho}\frac{\partial^2 \rho}{\partial t^2}. \tag{5}$$

After the double time derivative of the equation (3) and some simplifications we obtain

$$\frac{\partial^2 p}{\partial t^2} = c^2 \cdot \frac{\partial^2 \rho}{\partial t^2}, \tag{6}$$

where $c^2 = p\kappa/\rho$ is defined as the speed of sound in gas at the standard Earth sea-level conditions (at low gas pressures and densities). Finally, after substitution of the term (6) into (5) we obtain the partial differential equation that describes the acoustic waves in the time domain

$$-\text{div}\left(\frac{1}{\rho}\text{grad}\ p\right) + \frac{1}{\rho c^2} \cdot \frac{\partial^2 p}{\partial t^2} = 0, \tag{7}$$

3. Illustrative example

Consider a semi-circular diffuser in free space in front of the planar signal source. The left part of Fig. 1 shows the principal arrangement with the geometrical dimensions. The problem is considered planar. The basic dimensions of the impedance-matched area (representing the free space) are 5 m and 8 m, respectively. The source of the signal has a square platform with dimensions of 0.2 m and the signal spreads from one side. It is located at the distance of 5 m form the reflective element whose radius is 0.3 m. There are also points (probes $0-6$) around the diffuser (marked by small black dots) along the radius of 2 m, where the values of acoustic pressure are investigated.

3.1. Boundary conditions and environment properties

The solution of partial differential equation (7) requires correct boundary conditions. These are defined by either the values or normal derivatives of the acoustic pressure p along particular edges of the area of solution.

The boundary conditions for reflective surfaces, axis of symmetry and impedance-matched boundary are specified by the Neumann boundary condition

$$\frac{1}{\rho} \cdot \frac{\partial p}{\partial n_0} = D_{\mathrm{n}}\,, \tag{8}$$

where the values of function D_{n} are defined according to the right part of Fig. 1.

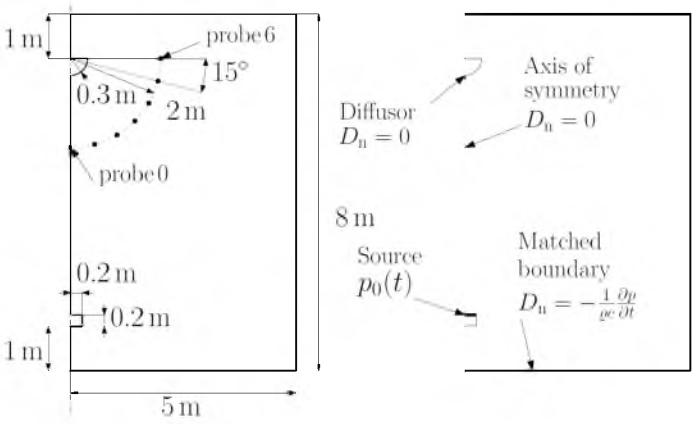

Fig. 1. Left: geometrical arrangement of the system, right: boundary conditions

The surface source of signal is defined by Dirichlet boundary condition

$$p = p_0(t), \tag{9}$$

where $p_0(t)$ is a function describing the source of the signal.

The illustrative example is solved in the air with the following parameters: the specific mass density $\rho = 1.2\,\mathrm{kg\ m^{-3}}$ and speed of sound $c = 343\,\mathrm{m\ s^{-1}}$ (for the ambient temperature $T_0 = 20\,°\mathrm{C}$).

3.2. Gauss monocycle pulse

The function of the Gauss monocycle pulse is in the solved task defined as the Dirichlet boundary condition to the boundary related to the source of signal. The time dependence could be explained using the equation

$$p_0(t) = A \cdot \mathrm{e}^{-\pi^2 \cdot f_0^2 \cdot (t - 1/f_0)^2}. \tag{10}$$

Here, the symbol A [$\mathrm{m^3\ s^{-1}}$] is the amplitude of the pulse and f_0 [Hz] denotes the pulse bandwidth. The Gaussian pulse and its derivative for the amplitude A = 100 $\mathrm{m^3\ s^{-1}}$ and frequency f_0 = 500 Hz are depicted in Fig. 2.

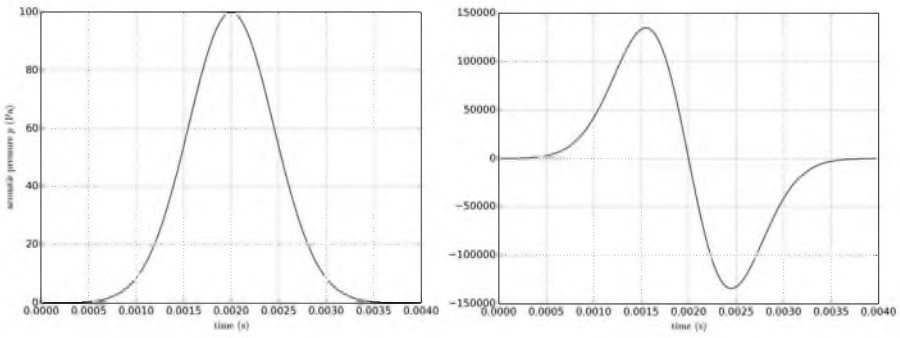

Fig. 2. Left: Gaussian pulse, right: derivative of Gaussian pulse

The parameter f_0 is crucial for the calculation of the mesh element size according to the term $f_0 = c / (N h)$, where h is a typical mesh element size and N is the number of elements per wavelength. For our purposes $N = 4$ as an acceptable value with sufficient accuracy, so that the value of h is 0.1715 m. The maximum surface of the triangle shape mesh elements will be in this case about 0.013 $\mathrm{m^2}$.

For the convergence of the solution we define the CFL number as the fraction of an element the wave travels in a single time step with respect to length h, in other words, as the ratio

$$\mathrm{CFL} = \frac{c \cdot t_{\mathrm{step}}}{h}. \tag{11}$$

The typical value of the CFL number in case of the 2nd order elements is about 0.1 for reaching the convergence. This value of CFL leads to the length of the time step 0.05 ms.

4. Numerical solution

The solution of (7) was performed using the higher-order finite element method (*hp*-FEM). This method is implemented in the C++ library Hermes [3] developed by hpfem.org group and it is used in Agros2D application [4] developed by the group at the University of West Bohemia in Pilsen. Agros2D allows solving partial differential equations and exhibits a lot of unique features suitable for numerical modeling (interactive geometry creation, support of curvilinear elements and hanging nodes, scripting support in Python language, particle tracing and much more).

4.1. Convergence of the results on the example with 500 Hz bandwidth

The computations were performed using the properties of air and mesh which have been mentioned in subsection 3.2. Figure 3 shows the dependence of the selected CFL numbers on the results of the numerical simulations. The results corresponding to the CFL numbers 0.05 and 0.025 are almost identical. The boundary securing the convergence of results corresponds to the values ranging from 0.05 to 0.1. In principle, higher CFL numbers lead to an inaccurate solution.

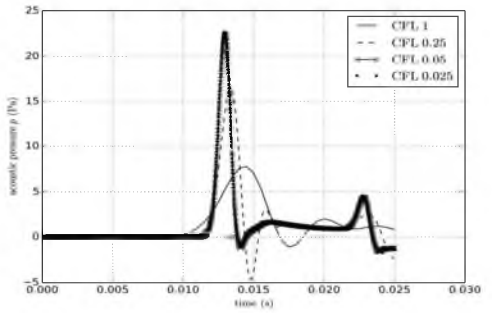

Fig. 3. Time dependence of acoustic pressure to CFL number at place of probe 0

The result of the numerical solution in the time domain is the time evolution of the distribution of acoustic pressure p in the whole area of solution in the above time range. This distribution at three selected time instants is shown in Fig. 4.

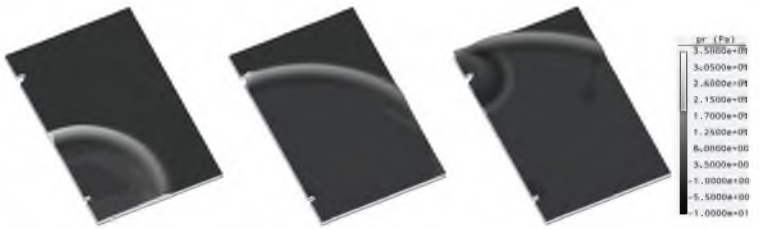

Fig. 4. Distribution of acoustic pressure for the pulse bandwidth 500 Hz in time steps: left - 10×10^{-3} s, middle- 18×10^{-3} s and right- 22×10^{-3} s

4.2. Results of the pulse simulations with 1 kHz bandwidth

Obtaining an accurate solution at high frequencies (while keeping the CFL number on a sufficiently low value) requires a very fine mesh. In this case we use the advantages of hp-FEM. The elements covering the area are set to the order of 3 and their maximum surface could be set to a lower value. In our case, it was set to 0.03 m^2 (while according to the calculations in previous case it should be set to 0.003 m^2). The transient was calculated for time ranging from 0 s to 0.025 s with the length of the fixed time step $\Delta t = 3.125 \times 10^{-5}$ s. The CFL number is in this case 0.04. The time-dependent values of the acoustic pressure at the position of probes 0, 3 and 6 are depicted in Fig. 5.

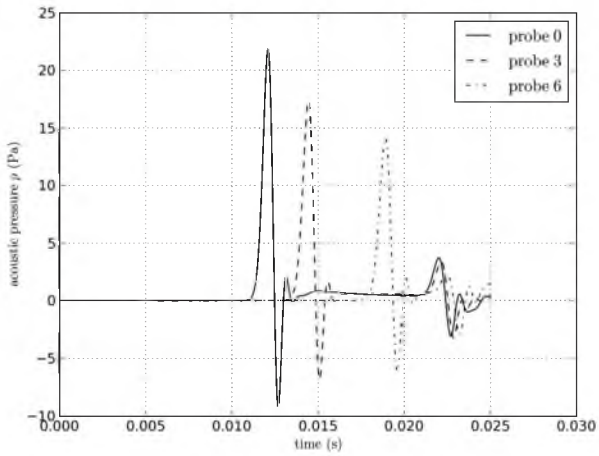

Fig. 5. Time dependence of acoustic pressure at place of selected probes

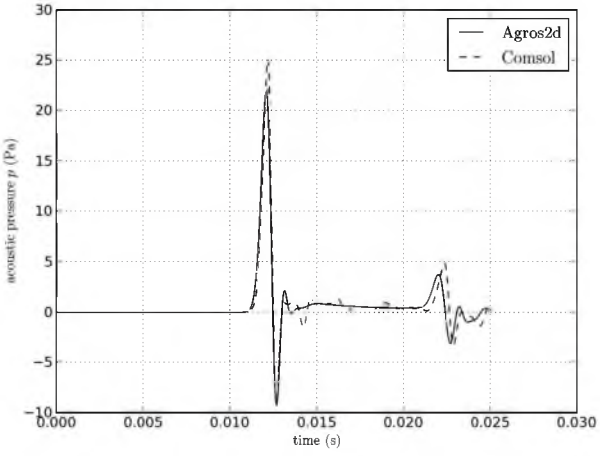

Fig. 6. Comparison of time dependence of acoustic pressure at probe 0 obtained by both used codes

The same example was also solved by the commercial software COMSOL Multiphysics 4.2 [5] using the module called TRANSIENT PRESSURE ACOUSTICS. The goal was to verify the results obtained by the Agros2D application. Due to different algorithms for meshing the definition area, the resultant mesh differed in this case substantially. Nevertheless, the dimensions of the largest elements of the mesh were the same as in case of the Agros2D code. The time step in COMSOL was used adaptively, with the maximum length 8.79×10^{-5} s.

The comparison of results at the probe 0 placed on the axis of symmetry is carried out in Fig. 6. The curves calculated by Agros2D and COMSOL are very similar. The small differences are mainly caused by the accuracy of the numerical solution. Due to the shape of the Gauss monocycle pulse, the results from Agros2D could be improved by using of adaptive time stepping.

5. Conclusion

Modelling of acoustic transient filed was performed by using the appropriate acoustic module of Agros2D application. It has been tested on several examples and in all cases the results were consistent with the results obtained using the commercial software COMSOL Multiphysics. This paper describes the results from the semi-circular acoustic diffuser reflecting a signal in the form of the Gauss monocycle pulse.

The future work in this field will be focused on the correlation of signals for obtaining the required time window for the next signal processing (discrete Fourier transform and calculation of diffusity and scattering coefficient) and the verification of results by experimental measurements.

Acknowledgement

This work was supported by the Ministry of Industry and Trade of the Czech Republic under the project FR-TI4/569: Development of a new generation of acoustic diffusers and their modelling and the University of West Bohemia in Pilsen under the project SGS-2012-039.

References

[1] Cox J. T., P. D'Antonio, Acoustic Absorbers and Diffusers Theory. Design and Application, Taylor & Francis Group, 2009.

[2] Rossing T. D., Springer Handbook of Acoustics. Springer Science + Business Media, LLC New York, 2007.

[3] Solin P. et al, Hermes – Higher-order Modular Finite Element System, http://hpfem.org.

[4] Karban P. et al, Agros2D – Multiplatform C++ Application for the Solution of PDEs, http://agros2d.org.

[5] COMSOL Multiphysics, http://www.comsol.com.